

Sensitivity of dim 8 EFT operators to resonance signals in Vector scattering boson scatterings

Bachelor-Arbeit
zur Erlangung des Hochschulgrades
Bachelor of Science
im Bachelor-Studiengang Physik

vorgelegt von

Georg Schmieder
geboren am 14.10.1996 in Oschersleben

Institut für Kern und Teilchen Physik
Fakultät Physik
Bereich Mathematik und Naturwissenschaften
Technische Universität Dresden
2022

Eingereicht am xx. Monat 20xx

1. Gutachter: Dr. Frank Siegert
2. Gutachter: Prof. Dr. Arno Straessner

Summary

Abstract

English:

Abstract

Deutsch

Contents

1	Introduction	7
2	ATLAS Detektor	9
2.1	ATLAS	9
3	Theoretical Foundation	11
3.1	Effective Field Theory	11
3.1.1	Fermi Theory on the example Tau Decay	11
3.1.2	Standard Model Effective Field Theory(SMEFT)	14
3.1.3	EFT validity and unitarity violation	15
3.2	BSM Theories	16
3.3	Vector Boson Scattering	18
4	Event Selection	21
5	Results	25
6	Summery and Outlook	31
	List of Figures	33
	List of Tables	35
6.1	Appendix	36

1 Introduction

Theoreticlay SM complete but not experimantaly

2 ATLAS Detektor

CERN may be the most famous scientific institution in the World. The Large Hadron Collider(LHC) build in 2008 is the largest circular collider in the World. Famous for the first discovery of the Higgs-Boson the two-ring-superconducting-hadron accelerator and collider are where in a 26.7 km tunnel. This Technological marble is only possible because of thousands of engineers, computer scientists and physicists. Four large detectors ALICE, ATLAS, CMS and LHC and other smaller experiments are connected to the LHC. The LHC aims for a collision energy of 14 TeV as of now Run-II achieved 13 TeV by accelerating particle beams up to 6.5 TeV. The Number of events per second N is given by:

$$\frac{dN}{dt} = L\sigma \quad (2.1)$$

σ is the cross-section of particles and L the luminosity defined as:

$$L = \frac{N_b^2 n_b f \gamma}{5\pi \epsilon_n \beta^*} F \quad \text{with} \quad F = \left(1 + \left(\frac{\theta_c \sigma_z}{2\sigma^*}\right)^2\right)^{-\frac{1}{2}} \quad (2.2)$$

N_b number of particles per bunch

n_b number of bunches

ϵ_n normalized transverse beam emittance

β^* beta function at collision point

F Luminosity correction in the interaction point based on the crossing angle

With the start of Run-3 on April 22, 2022 a collision energy of 13.6 TeV is expected.

2.1 ATLAS

ATLAS the largest general-purpose detector is a part of the LHC experiments with more than 5500 scientists working on ATLAS experiments worldwide.

Magnet System

The Magnet System creates the Magnetic field that bends the trajectory of the incoming particles in order to measure the momentum of said particles. For this purpose two superconducting Toroids create a magnetic field $B = 2$ T. The momentum can be calculated from the curvature r due to the Lorenz force.

$$r = \frac{p}{qB} \quad (2.3)$$

where $p = \gamma mv$ is the relativistic momentum and q the charge of the particle. High momentum-particles result in small curvature while low-momentum particles show a greater curvature.

Inner Detector

The inner detector consists of three Subdetectors. The ATLAS-Pixel detector is the innermost part surrounded by the Semiconductor Tracker (SCT) providing additional data for the curvature calculation. The outermost layer is the Transition Radiation Tracker (TRT). Transition radiation is to differentiate between fermions and hadrons.

Calorimeters The electromagnetic Calorimeter and the Hadron calorimeter make up the calorimeter system. Particles that interact via electromagnetic force are measured in the electromagnetic calorimeter. Electrons or photons create particle showers in the electromagnetic calorimeter and no showers in the hadronic calorimeter while hadrons show traces in both and showers mostly in the hadronic calorimeter. This happens because hadrons have a higher mass and the cross-section is inverse proportional to the mass of the particle.

Muon Spectrometer

3 Theoretical Foundation

3.1 Effective Field Theory

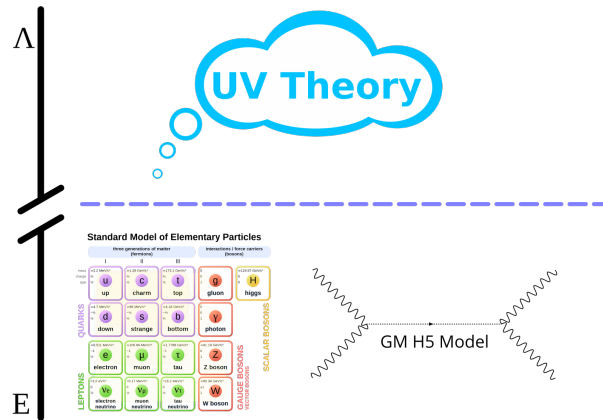


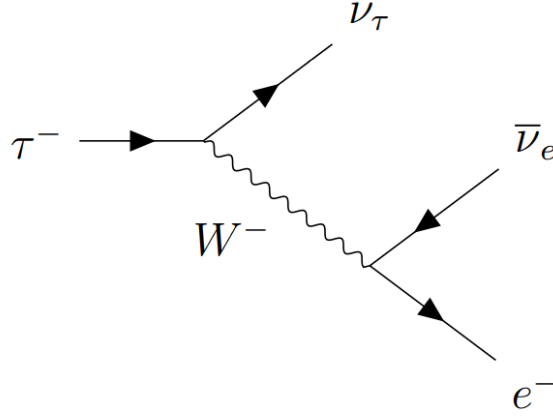
Figure 3.1: Sketch of the Basic EFT concept with the low energy observer having energy E and cutoff at Λ . The SM and BSM theory(here GM H5 Model) are combined in the Effective Field Theory. [Bri17]

With the Standard Model Physicist try to describe the elementary Particles and interactions. It is successful in describing most processes in Biology, Chemistry, and Physics. But the Standard Model is still incomplete. It can't describe Phenomenons like Gravity, Neutrino Masses, Matter-Antimatter asymmetry etc. This is where effective field theory comes in. Here we look at the Standard Model as a low energy approximation of an underlying Ultraviolet Theory (figure 3.1).

3.1.1 Fermi Theory on the example Tau Decay

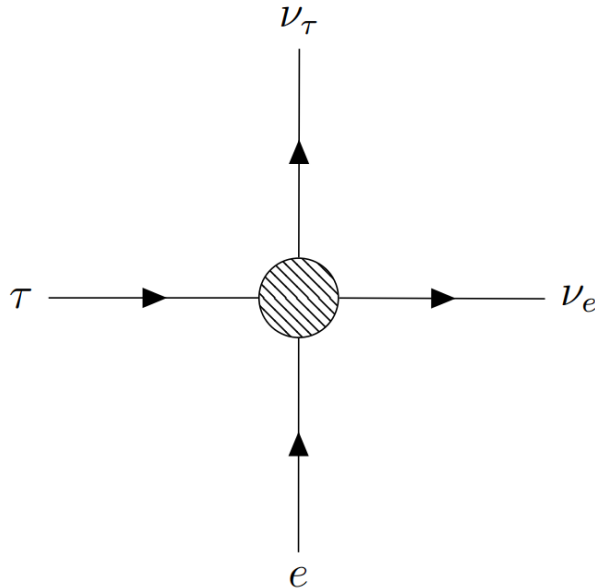
Enrico Fermi proposed 1933 the Fermi Theory in order to describe the β -decay. His theory was able to describe the weak coupling quite well without the former knowledge about the W^\pm -Boson which was only later theorized in 1968 by Steven Weinberg, Sheldon Glashow and Abdus Salam. The W^\pm -Boson was finally discovered in 1983. 50 years after Fermi's first successful description of an Interaction involving the W^\pm -Boson. Today we would call the Fermi theory the low-energy effective field theory of W^\pm -Boson. Let us now try to create our own Fermi Theory but instead of describing the β decay we will look at the τ -decay specifically the decay mode $\tau \rightarrow \nu_\tau e^- \nu_e$. Even though we are technically cheating since Fermi didn't have

our knowledge about the tensor structure of the Weak interaction in Quantum Field Theory or our knowledge about Feynman diagrams. We will start by drawing the Feynman Diagram and writing down the Matrix element.



$$-i\mathcal{M}_{fi} = \left[\frac{g_W}{\sqrt{2}} \bar{u}(k_{\nu_\tau}) \frac{1}{2} \gamma^\mu (1 - \gamma^5) u(k_\tau) \right] \frac{g_{\mu\sigma} - \frac{k_\mu k_\sigma}{m_W^2}}{k^2 - m_W^2} \left[\frac{g_W}{\sqrt{2}} \bar{u}(k_e) \frac{1}{2} \gamma^\sigma (1 - \gamma^5) v(k_{\bar{\nu}_e}) \right] \quad (3.1)$$

In most low energy decay processes the momentum of the intermediate W^- -Boson is small compared to its mass. Therefore, we can approximate the propagator(3.2) in Orders of the momentum k but we will be writing it in the Matrixelement in Orders of mass since these are more interesting to us. In the Feynman Diagramm this can be expressed by collapsing the propagator into a single Vertex.



$$\frac{-ig_{\mu\sigma} - \frac{k_\nu k_\sigma}{m_W^2}}{k^2 - m_W^2} \xrightarrow{|q|^2 \ll m_W^2} \frac{ig_{\mu\sigma}}{m_W^2} \left(1 + \frac{k^2}{m_w^2} + \frac{k^4}{m_W^6} + \mathcal{O}(k^6) \right) \quad (3.2)$$

$$\Rightarrow i\mathcal{M}_{fi} = \frac{g_W^2}{8m_W^2} [\bar{u}(k_{\nu_\tau})\gamma^\mu(1 - \gamma^5)u(k_\tau)] g_{\mu\sigma} [\bar{u}(k_e)\gamma^\sigma(1 - \gamma^5)v(k_{\bar{\nu}_e})] + \mathcal{O}(m_W^4) \quad (3.3)$$

Let us now compare our result with the result Fermi would have gotten if he knew about the parity violation discovered by Wu in 1957.

$$i\mathcal{M}_{fi} = \frac{G_F}{\sqrt{2}} [\bar{u}(k_{\nu_\tau})\gamma^\mu(1 - \gamma^5)u(k_\tau)] g_{\mu\sigma} [\bar{u}(k_e)\gamma^\sigma(1 - \gamma^5)v(k_{\bar{\nu}_e})] \quad (3.4)$$

With $G_F \approx 4.5437957 \times 10^{14} J^{-2}$ being the Fermi constant which is typically measured in the muon decay. The $1/\sqrt{2}$ is added in order to not change the numerical value of G_F while considering the parity violation. From equation 3.3 and 3.4 we get the following result.

$$\frac{G_F}{\sqrt{2}} = \frac{g_W^2}{8m_W^2} \quad (3.5)$$

Defining the expansion scale $\Lambda = m_W$ and the Wilson coefficient $c = \frac{g_W^2}{8}$ we can see that the Matrix element has dimension 2. With this we can also write down a new effective Lagrangian without the W^\pm -Boson but. The EFT described has to contain the tau, electron, their respective neutrino fields as well as the Interaction Lagrangian.

$$\mathcal{L}_{EFT} = \frac{c}{\Lambda^2} (\bar{\nu}_\tau \bar{\gamma}_\rho \tau) (\bar{e} \gamma_\rho \nu_e) + \mathcal{O}(\frac{1}{\Lambda^4}) \quad (3.6)$$

Our Fermi Theory is only valid for low energies since Scattering Amplitude from the Standard Model and the EFT would start to diverge once the Energy gets close to the mass of the W^\pm -Boson. The m_W defines the validity scale of the EFT in this case the Fermi Theory. For Energies higher than m_W the Fermi Theory is no longer valid. We can increase the validity scale by including terms of higher dimension in Λ . In this example we derived the Matrix element from the SM and then compared the result with the result from Fermi in order to determine $\frac{c}{\Lambda}$. This requires knowledge about the UV theory which is not accessible in low-Energy Measurements. As a result we have to make assumptions about a UV Theory in order to construct the right EFT.

3.1.2 Standard Model Effective Field Theory(SMEFT)

The Name suggests The SMEFT aims to extant the Standard Model. Except the g-Faktor of the Myon the Standard Model has been robust without meaningful deviations from Experimental Measurements. There using a theory that keeps the $SU(3) \times SU(2) \times U(1)$ symmetry with the Higgs field breaking gauge symmetry is desirable. Therefore, we construct the Lagrangian from the gauge invariance for Standard Model fields but allow arbitrarily large mass dimensions. With that any SMEFT Lagrangian can be written as:

$$\mathcal{L}_{SMEFT} = \mathcal{L}_{SM} + \frac{1}{\Lambda} \mathcal{L}_5 + \frac{1}{\Lambda^2} \mathcal{L}_6 + \frac{1}{\Lambda^3} \mathcal{L}_7 + \frac{1}{\Lambda^4} \mathcal{L}_8 + \dots \text{ with } \mathcal{L}_i = \sum_i c_i^D \mathcal{O}_i^D \quad (3.7)$$

The operators \mathcal{O}_i are constructed from the Gauge invariance of the SM fields while the Wilson coefficients c_i contain the information on heavy degrees of freedom. Normally the heavy degrees of freedom are integrated out to have a renomilazible Theory but are needed to describe high energy Particles. We get the Wilson coefficients from the operator product expansion in 3.7 as shown in the Fermi Theory(3.1.1). For a characteristic heavy scale Λ the operators are ordered by there dimension d_i fixing the dimension of their respective coefficients.

$$[\mathcal{O}_i] = d_i \longrightarrow c_i \sim \frac{1}{\Lambda^{d_i-4}} \quad (3.8)$$

The Leading order $D = 4$ (marginal operator) term in 3.7 is the SM Lagrangian while deviations of the SM are described by operators with a dimension $D > 4$ also called Irrelevant operators since they are suppressed by teh scale E/Λ . Even though they are called irrelevant they often contain important information for processes with high energy. In a Fermi Theory these contain information about processes with leading order flavour-change. Relevant operator $D < 4$ become relevant for energies close to the validity scale and only EFT's with relevant and marginal operators are normalizable making the predictions valid up to E/M .

Using knowledge about SM field and known symmetries one can construct an operator basis. All allowed invariant structure are found using the SM fields and their symmetries at a dimension D . Removing all terms from the S-matrix that would result in the same Physics provides the basis. The General choice of basis in the search for new Physics is the Warsaw basis [] other basis can be chosen as Physics should be basis indepentent. In VBS processes the Eboli basis is commonly used because the operators can be categorized in Longitudinal Operators only containing covariant derivatives D^μ and a Higgs doublet fields Φ , Transverse operators only containing field strength tensors $\widehat{W}_{\mu\nu}$ and Mixed operators containing combinations. Most of the operators can be discarded since they don't contribute to WZ processes leaving only six

dimension-8 operators.

$$\text{Longitudinal: } \mathcal{O}_{S,1} = [(D_\mu \Phi)^\dagger D_\mu \Phi] \times [(D^\nu \Phi)^\dagger D^\nu \Phi]$$

$$\begin{aligned} \text{Mixed: } \mathcal{O}_{M,0} &= Tr[\widehat{W}_{\mu\nu} \widehat{W}^{\mu\nu}] \times [(D_\beta \Phi)^\dagger D^\beta \Phi] \\ \mathcal{O}_{M,1} &= Tr[\widehat{W}_{\mu\nu} \widehat{W}^{\mu\beta}] \times [(D_\beta \Phi)^\dagger D^\mu \Phi] \end{aligned}$$

$$\begin{aligned} \text{Transverse: } \mathcal{O}_{T,0} &= Tr[\widehat{W}_{\mu\nu} \widehat{W}^{\mu\nu}] \times Tr[\widehat{W}_{\alpha\beta} \widehat{W}^{\alpha\beta}] \\ \mathcal{O}_{T,1} &= Tr[\widehat{W}_{\alpha\nu} \widehat{W}^{\mu\beta}] \times Tr[\widehat{W}_{\mu\beta} \widehat{W}^{\alpha\nu}] \\ \mathcal{O}_{T,2} &= Tr[\widehat{W}_{\alpha\mu} \widehat{W}^{\mu\beta}] \times Tr[\widehat{W}_{\beta\nu} \widehat{W}^{\nu\alpha}] \end{aligned}$$

3.1.3 EFT validity and unitarity violation

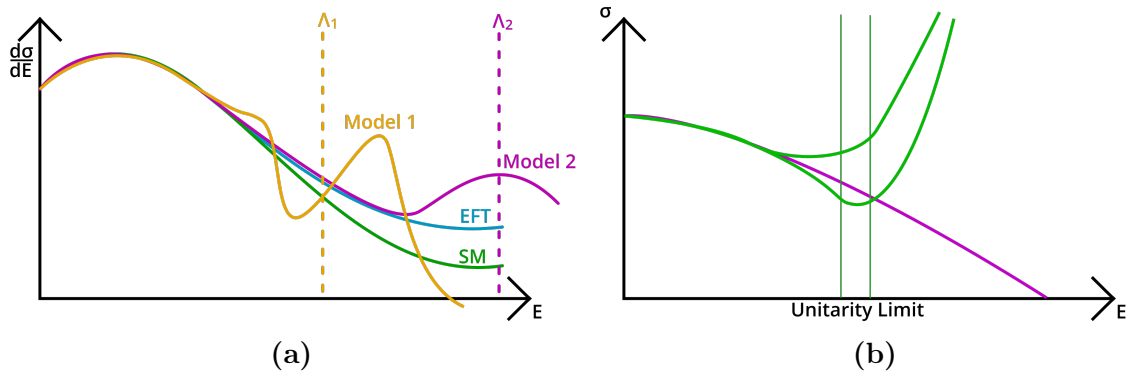


Figure 3.2: a) Not all Models can be fitted using EFT only ones with energy scale higher than the SM b) Schematic of unitarity limits the energy range changes depending on the cutoff [MSz]

The time evolution of states in quantum mechanics is mathematically described by unitary operators. Time evolution without unitary operators is proposed in new approaches to quantum mechanics like Carl M. Bender's talk in 2021 at the TU-Dresden proposing a quantum theory including non Hermitian Hamiltonian. Unitarity was a decisive concept for the inclusion of the Higgs field in the SM as it restored unitarity at tree level. EFT isn't a complete theory by extending the SM, TGC and QGC processes are modified leading to unitarity violation. The expected behaviors of a Unitary EFT is $\text{dim-6 interference} > \text{dim-6 quadratic} \sim \text{dim-8 interference} > \text{dim-8 quadratic}$. This however is not the case as dim-8 operators cause the Scattering amplitude to grow asymptotically $\sim \Lambda^2$ eventually leading to unitarity violation 3.3. One can now apply a cutoff at the validity scale $M = \Lambda$ but in practice the value of Λ is unknown and can only be gained by analyzing data. This means that EFT predictions are only valid for an operator dependent unitarity limit. It should be noted that unitarity can be restored by using unitarisation. In ATLAS research the relatively simple K-matrix method is

common tool for unitarisation as shown in [Kil+15]. This however does not restore EFT validity and makes connecting EFT results to UV Theories harder. In conclusion the search for BSM effects using EFT is only possible in an Energy range as light states are not detectable and high Energy states are removed by the unitarity limit 3.2.

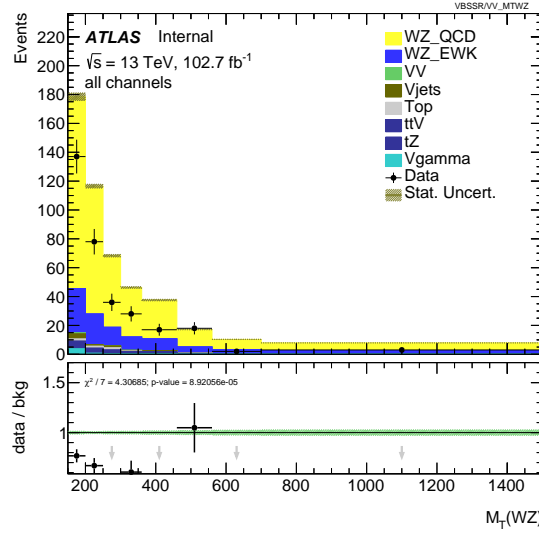


Figure 3.3: Comparison of interference term and quadratic term for the S1 parameters created with value $S1=128$. The quadratic term is bigger for higher energies since no unitarisation is used.

3.2 BSM Theories

In 2012 the last particle predicted by the SM was detected at CERN the Higgs Boson. Yet again proving the success of the SM. But this also means no more free parameters in the SM for new particles. All interactions found obey the local $SU(3) \times SU(2) \times U(1)$ gauge symmetries and later data only strengthens the SM prediction. While no data was found suggesting inconsistencies with the electroweak symmetry breaking $SU(2) \times U(1) \rightarrow U(1)$ and no new exotic particles are found between 0-2 TeV 3.5. This means physicist have to search for new interactions considering different interaction ranges and strengths(Figure 3.4).

- (a) Considerably weaker than gravitation with infinite range
- (b) Shorter range than the weak interaction of any strength
- (c) Range between weak interaction and nuclear force and considerably weaker than the weak interaction

There are various methods for finding BSM particles and as many theoretical models for new interactions, but these can generally be broken down in three categories.

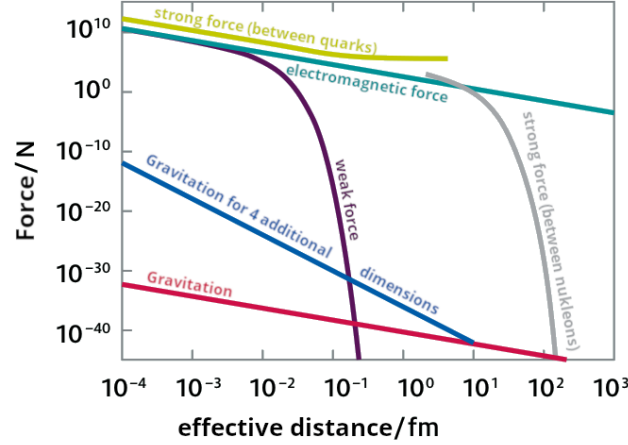


Figure 3.4: Interaction strength for different ranges of the Fundamental interactions. Although the Nuclear force isn't a fundamental it is shown in order to visualize point (c). [Teilchenwelt]

The Model specific search where one takes a well-defined model often describing a complete UV theory and try's to find the predicted particles in measurements. The most popular example for this is the Supersymmetry(SUSY) which is often associated with the search for Dark Matter and adds a wide range of different particles. In the search for Dark Matter one would look for example look for missing transverse momentum in top quark interactions or look for resonance with the so-called two Higgs doublet models.

Another way of looking for new physics is by using simplified Models. Here one takes a well-defined model in order to describe some aspects or specific phenomenon of the UV Theory. Again a good example comes from dark matter physics the beautifully named neutralino in Minimale Supersymmetry Standard Model(MSSM) with MSSM being a low energy model of the SUSY. Here the for neutralinos are electrically neutral fermions with a mass over 300 GeV and conserves the hypothetical R-parity in MSSM. Compared to the Model specific search the result would give evidence only for the R-parity and the neutralino but not for other aspects of SUSY.

These first two methods depend entirely on a theoretical model. Granted these models are often well motivated by known physics or mathematical structures. But history has shown multiple times that experiments can produce unexpected results. As a recent example being the accelerating expansion of the Universe by some so-called Dark Energy. Unfortunately unexpected results are often not described by existing models, therefore a model independent search has to be done and EFT is the primary tool for this in particle physics. Taking a look at the Fermi Theory (section 3.1.1) again one will realize that Fermi's Theory was able to approximate the weak interaction but isn't able to describe the structure of weak interactions.

Only using Fermi's Theory one would not be able to describe CP-Violation. Generally describing an exotic interaction using EFT one can only predict low order processes, but the low energy observer can't make predicting as to what he is actually describing. The results can then be used to construct an appropriate model or match an existing one and use the first to methods to validate this model.

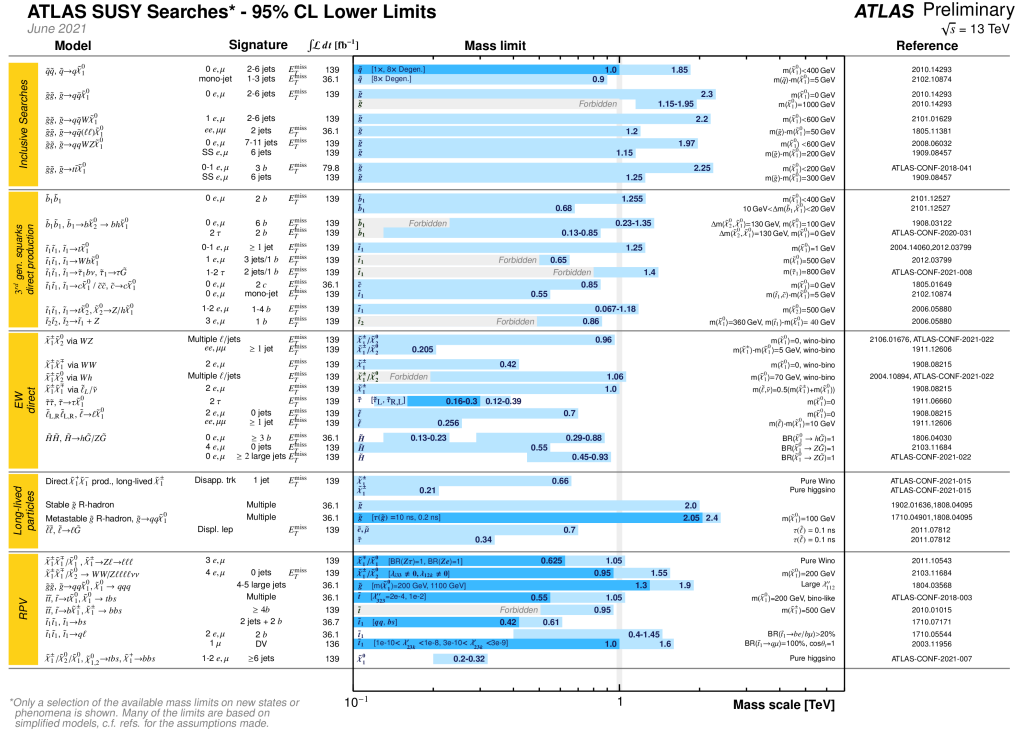


Figure 3.5: Example for SUSY as BSM Model. All particles shown here have been rejected as they should have been found using described methods in BSM search. []

3.3 Vector Boson Scattering

Vector Boson Scattering(VBS) refers to the scattering of any electroweak gauge Boson $V=W^\pm, Z, \gamma$. This Definition includes diboson processes which makes it necessary to specify the finale state for VBS and diboson processes. The VBS finale state $VVjj$ is characterized by the two Bosons and two jets while diboson processes finale state only contains two Bosons VV in the finale state. Since gauge bosons have a short half-life of $3 \cdot 10^{-25}$ s one needs to include the decay of the outgoing boson leading to the full process $qq \rightarrow VVjj \rightarrow 4ljj$ shown in figure 3.6. In leading order only quark-initiated diagrams produce vector bosons. These quarks are shifted by a small angle away from the beam axis resulting in the for the VBS process characteristic tagging jets. The couplings a to e in 3.6 are all electroweak interactions and based on there coupling structure produce a squared matrix element $|M^2| \propto \alpha_{EW}^6$. The α_{EW} stands for the combined coupling strength of the electroweak and electromagnetic interactions. These

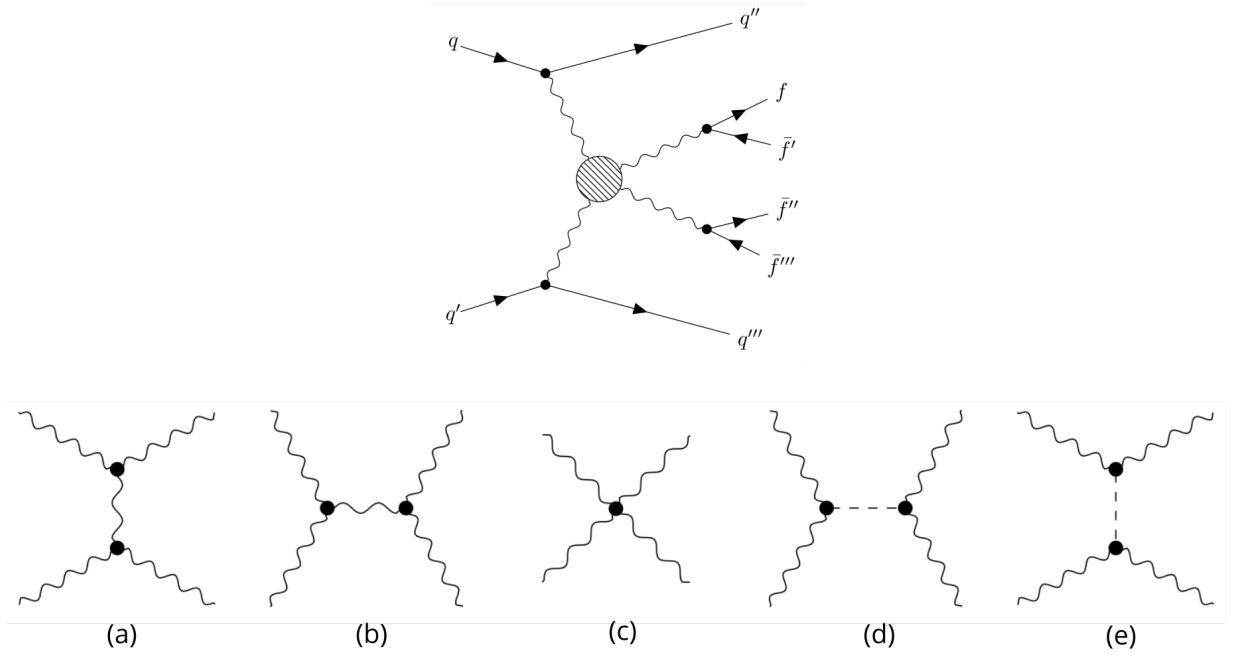


Figure 3.6: Structure of Full VBS process $qq \rightarrow VVjj \rightarrow 4ljj$ with two of the four leptons having a charge. The circle stands for the processes a to e which come from the non-Albanian gauge group $SU(2)$ for weak interactions in leading order $VV \rightarrow VV$ processes.[Bit20]

couplings can also be achieved by coupling structure $|M^2| \propto \alpha_{EW}^4 \alpha_S^2$, but these couplings however do not contribute to VBS processes. In the signal for VBS processes the diagrams with less than six electroweak diagrams are considered as Background defining the $VVjj - EW6$ processes. Some examples for the these processes can be seen in 3.7. How these processes are selected will be discussed in the following chapter. The $W^\pm Z$ processes is dominated by EW and QCD interactions specifically the EFT Terms are only accounted for in the EW interactions.

Multiple factors make the study of VBS processes interesting. VBS processes are only accessible from LHC Run-II and forward making them more relevant in the future. The appearance of both triple and quadratic gauge couplings lead to interesting studies polarization, gauge invariance, unitarity and Higgs physics. The distinct two jet finale state makes the selection of VBS process relatively easy leading to a small Background estimation. In BSM both properties are relevant as new Models often include triple and quadratic gauge couplings and without knowing the underlying theory it is hard know the impact of an BSM theory on the Background. In EFT triple gauge coupling are essential for analysis on dim-6 operates and quadratic gauge coupling for studying dim-8 operators. The accessibility of a variety of couplings and the fact that no BSM theory to date fully describes anomalous couplings motivate

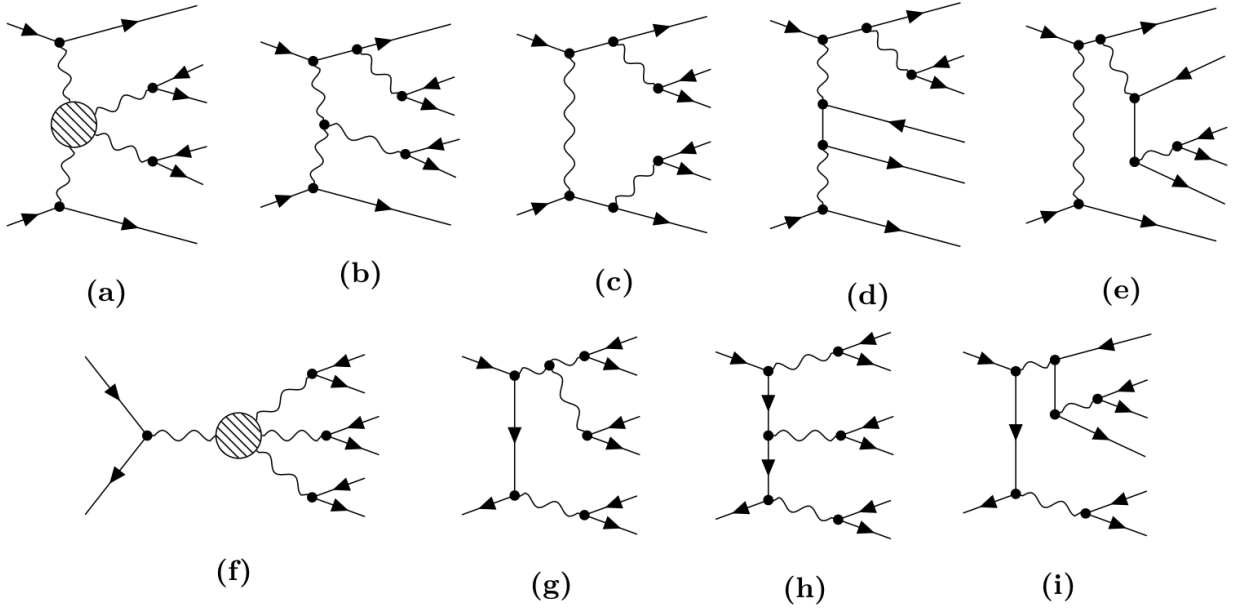


Figure 3.7: Example Feynman diagrams for VVjj-EW6 processes. The dashed circle stands for the Feynman diagrams a-e in Figure 3.6

the research on resonances in VBS using EFT.

4 Event Selection

Event selection criterion	llvjj region	WZjj region	VBSSR
Event cleaning	✓	✓	✓
GoodRunList	✓	✓	✓
Trigger	✓	✓	✓
Primary Vertex	✓	✓	✓
llvjj finale state			
≥ 2 jets	✓	✓	✓
≥ 3 Z-Analysis leptons	✓	✓	✓
One SFOC pair	✓	✓	✓
l_W is in W-Analysis selection	✓	✓	✓
Transverse momentum of leading leptons			
$p_T(l) > 25(27)GeV$	✓	✓	✓
Transverse momentum of subleading jet			
$p_T(j_2) > 40GeV$	✓	✓	✓
$M_T(W) > 30GeV$		✓	✓
$ M(ll) - 91.1876GeV < 10GeV$		✓	✓
four Baseline leptons veto		✓	✓
b-jet veto		✓	✓
$M(jj) > 500GeV$			✓
$\Delta Y(jj) > 2$			✓

Table 4.1: Schematic view of cuts applied in different phase space regions. [Bit20]

Event Selection is done in order to decrease background and get a clean signal process. VBS processes have a small cross-section around 1 fb resulting in a small event count. In the 2015 and 2016 ATLAS run with 36 fb^{-1} not even 100 events produce VBS processes. Therefore one has to carefully select Events in order to get a meaningful signal process. The Event Selection is implemented as described in [Bit20] using the Common Analysis Framework(CAF). The Object selection however was already done in ELCore and account for the Event cleaning, GoodRunList, Trigger, Primary Vertex in Table 4.1 these can't be change in the CAF. Therefore, only the Event selection done in the CAF will be discussed. ELCore produces beam reconstruction level samples the Event Selection in the CAF is split into the three phase space regions llvjj, WZjj and the VBS signal region(VBSSR). Even though the regions are different the selection criteria overlap. The WZjj region use the selection criteria of the llvjj as base and introduces new selection criteria. The same is true for the VBSSR which builds upon the WZjj region as show in Table 4.1.

lllvjj region: Only events with 3 or more leptons that pass the Z-analysis are chosen. The Leptons are then assigned to the decaying gauge boson. For this same flavour and opposite charge(SFOC) leptons pairs are chosen. The pair with invariant mass close to the Z Boson mass is assigned to the Z-Boson. The highest transverse momentum p_T lepton from the remaining leptons is assigned to the W^\pm -Boson and required to pass de W-analysis. Chosen leptons need a transverse momentum $p_T > 25(27)$ GeV for the 2015(2016) campaign for the events to pass the trigger threshold. Events have to have two or more events in order to be selected. These jets need to have $p_T(j) > 40$ GeV to be considered as tagging jets.

WZjj region: Additinal cuts are applied for the WZjj region in order to maximise $W^\pm Z$ contribution in the lllvjj final state. Some Events line ZZ diboson production are expected to produce an additional lepton therefore a four lepton Baseline veto is applied. Events where the jet is considered a b-jet are discarded to minimize $t\bar{t}$ and other t-quark contributions. The Transverse mass of the W^\pm -Boson is required to be greater than $M_T(W) > 30$ GeV. The Z lepton pair has to have an invariant mass within 10 GeV of the Z-Boson mass $m_Z = 91.1876$.

VBSSR region: The resonance fitting is done in the VBSSR region. For this additional requirements must be added increasing WZjj-EW6 contribution compared to WZjj-EW4 and WZjj-EW5. For this two cuts for the tagging jets have to added. The invariant mass must be $M(jj) > 500$ GeV and the absolute rapidity difference hast be constraint $\Delta Y(jj) > 2$.

Figure 4.1 shows the cuts for the VBSSR region applied for the combined data from mc16d and mc16e with a combined luminosity of 102.7 fb^{-1} . These histograms will be combined to WZ + Background in the following Plots. Ideally one would use all campaigns mc16a, mc16d and mc16e with combined luminosity of 139 fb^{-1} to achieve the best statistic. For this Analysis the EFT Samples as well as the GM resonance samples have to be included resulting in to many Branches in the TQSampleTree than the current ROOT version 6.14.04 used by the CAF can process.

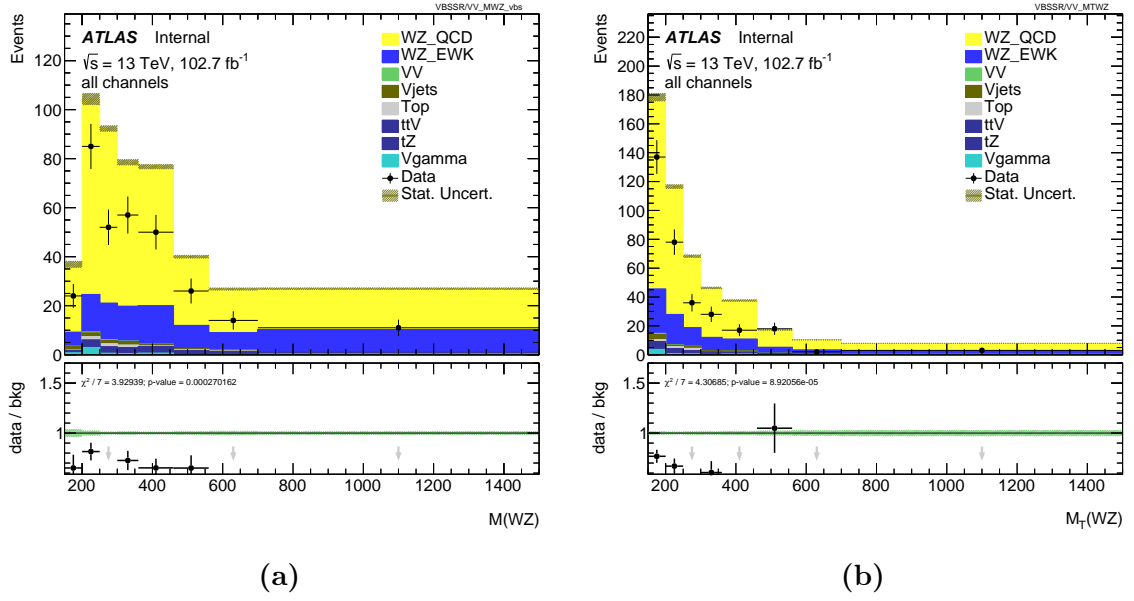


Figure 4.1: VBSSR region for a) invariant Mass, b) transverse mass. Showing reproduction of SM as well as the in section 3.3 discussed dominance of QCD and EW processes. VV, Vjets, Top, ttV, Vgamma, WZ_EWK, WZ_QCD are combined to 'WZ_SM + Background' in later plots. For the fits WZ_EWK is used as signal.

VBSSR	mc16d+mc16e	mc16a	SM
WZ QCD	356.8912 ± 2.4118	121.5475 ± 1.1721	144 ± 41
WZ EWK	91.2393 ± 0.4231	32.4363 ± 0.2522	24.9 ± 1.4
Background	27.2161 ± 2.0335	11.9691 ± 0.4701	31.1 ± 3.9
WZ SM + Background	475.3466 ± 3.2912	165.9529 ± 1.4050	200 ± 41

Table 4.2: Overview of Events in VBSSR region. mc16a is compared to the [STDM] for the reproduction of the SM EFT Limits. While the Resonance Fitting is done with the mc16e+mc16d data. The differences between the mc16a and the SM is like cause by some ELCore settings since the cuts possible in the CAF tool where replicated.

Operator	EFT Optimized binning		SM Optimized Binninig
	$M(WZ)$	$M_T(WZ)$	$M_T(WZ)$
S0	[-49 , 47.4]	[-46 , 44.1]	[-78 , 78]
M0	[-9.1 , 11.5]	[-9.3 , 9.65]	[-15 , 15]
M1	[-16 , 15.7]	[-15 , 14.4]	[-23 , 23]
T0	[-0.43 , 0.457]	[-0.38 , 0.325]	[-1.4 , 1.4]
T1	[-0.82 , 0.713]	[-0.72 , 0.682]	[-0.97 , 0.97]
T2	[-2.4 , 2.16]	[-2.2 , 1.96]	[-2.8 , 2.8]

Table 4.3: Asmieve fit Limits for SM data with 95% CL. Differences arise from the use of mc16e, mc16d data compared to the mc16a data and the use of an BSM search optimized binning compared to the SM optimized binning used in [NEEd OSurce]

5 Results

The EFT samples for each parameter S_0 , M_0 , M_1 , T_0 , T_1 , T_2 is fitted against the combined SM and GM Resonance data. It is assumed that the coefficients are only affected by aQCD couplings. Only one coefficient is fitted while the other coefficients are set to zero. As discussed in section 3.1 good fits are expected for sufficiently high resonance mass. The fit can't identify small energies or high energy with small cross-sections resonances as shown in 5.1.

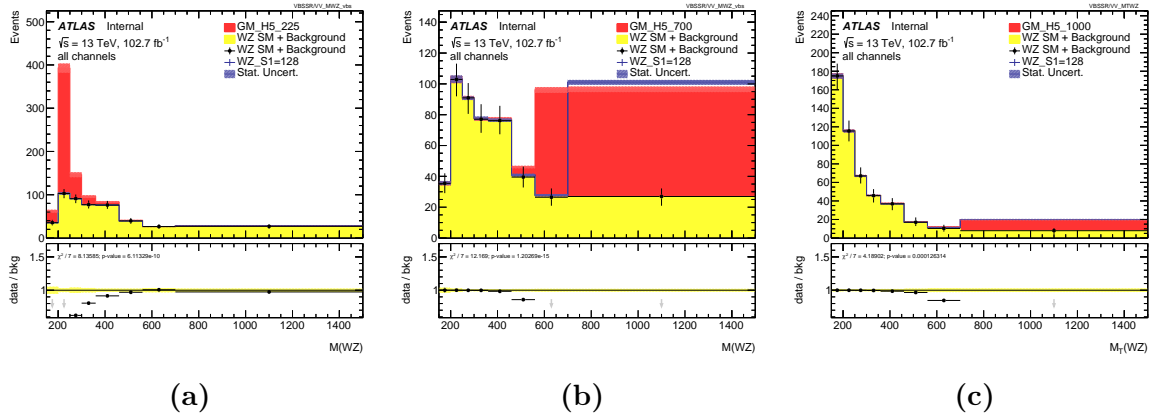


Figure 5.1: a) The invariant Mass of the resonance has approximately the same energy as the WZ peak but for the WZ peak the EFT prediction should be the SM therefore EFT can't describe the 225 GeV Resonance and the coefficient fit diverges. b) 700 GeV has a high cross-section and the energy is in the region where SM and EFT deviate therefore the coefficients can be fitted accurately. c) 1000 GeV the cross-section is too low the fit can produce a significant result even though the Resonance is in the right Energy region.

Evaluating which fit is good can be done qualitatively by simply looking at the invariant Mass plots if the EFT Sample scaled with the best fit value is able to describe the Resonance one can argue that the fit is good. But this is not accurately possible for resonances peaks that are higher energy than the WZ peak, but the start of the peak is still part of the WZ peak. For a quantitative analysis the significance quotient has to be calculated from the log-likelihood function $f(x) = -2\Delta\log(L)$. The significance can be calculated using $Z(x) = \sqrt{f(x)}$ resulting in $S = \frac{Z_{GM}(0)}{Z_{EFT}(0)}$. Here Z_{GM} is the significance when the GM Sample is used as coefficient in EFT-Fun and fitted with SM as measurement and as prediction. The Z_{EFT} is the fit of an EFT coefficient for the SM combined with the GM Model as measurement against the SM as prediction. $f(0)$ can be interpreted as the difference to the SM, if $f(0) = 0$ only the SM was measured and for $f(0) > 0$ the SM is excluded. The value of $f(0)$ can be read off from

the Log-likelihood-funktion in 5.2. The scale is dependent on the operator as well as the allowed range making it difficult to estimate a read off error. The error can be minimized by looking at positive and negative extrema and limiting the range to zero as well as the shape including both extrema. Since the likelihood-function continuous all plots give the same $f(0)$ value. All three ranges should be used in case only an extremum exists, or only one is recognized by the fit this is often the case for low resonance energies. Using this the error becomes small compared to the statistical errors. All EFT coefficients in 5.3 with $S > 0.8$ are able to reproduce the GM Model with a statistical significant greater than 80%. The result is independent of the resonance cross-section. This can be shown by scaling the resonance, in 5.4 the cross-section is scaled with 2 and 0.5 which results in equal significance compared to the non-scaled resonances. The cross-section can't be scaled higher without breaking the fitting-tool as the values get unreasonably high. In the invariant mass plot for 0.5 times the cross-section, the cross-section becomes too low to be picked up by the fitting tool but in the transverse mass plot the resonance was still picked up and accurately described even though the relevant energy doesn't change, and therefore the transverse mass plot becomes more interesting for low cross-section resonances. The 700 GeV sample has a significance of 0.7 – 0.8 making it irrelevant for this analysis but with the high dependence on the binning one may be able to get a significant result by optimizing the binning. The EFT limits for relevant resonance masses are shown in 5.1. The Limits for both extrema should be equivalent but the EFT-Fun only expects one extremum when fitting and therefore includes the second extremum in the 95%CL if the second extremum is too close to the first extremum. In order to find both extrema the range from a minimal range to zero for the negative extremum and from zero to a positive minimal range. The minimal range should leave space for the fit to find the best fit value. [T0 doesn't show this behaviour and combined with the in 5.4 shown ability to accurately describe low cross-section resonances may hint to a smaller impact of the Quadratic Term from T0.](#) A full set of all parameters and both invariant mass and transverse mass are shown in 5.5 and 5.6 for an 800 GeV resonance as this is the resonance with the lowest Energy and statistical significance. Other resonances are shown in the Appendix 6.1.

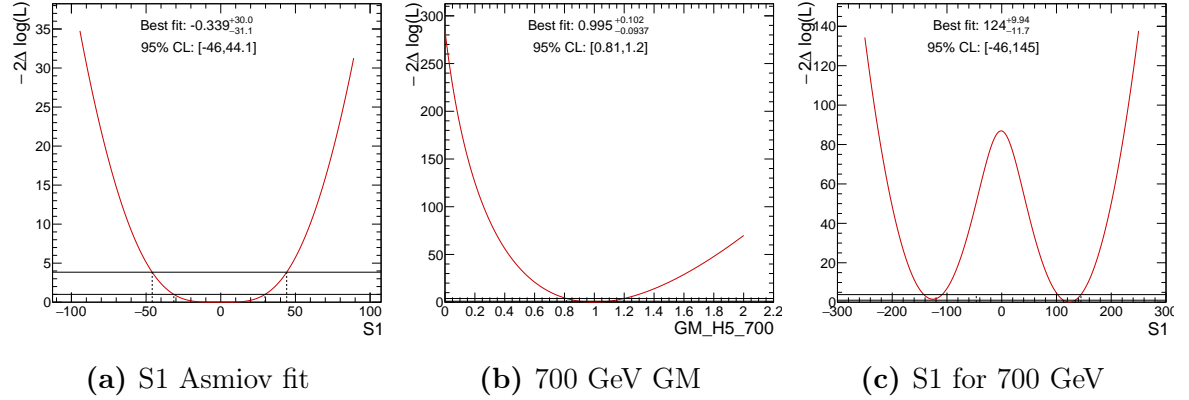


Figure 5.2: a) The best fit value is zero since the SM is reproduced in the asimov fit. c) The SM is excluded and two extra emerge from the inclusion of the quadratic operator therm.

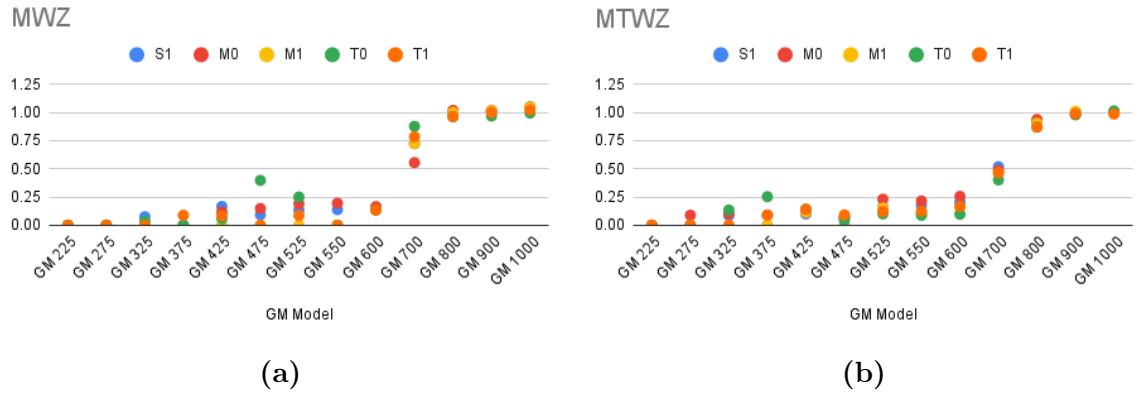


Figure 5.3: a) EFT coefficients significance for invariant Mass b) EFT coefficients significance for transverse Mass

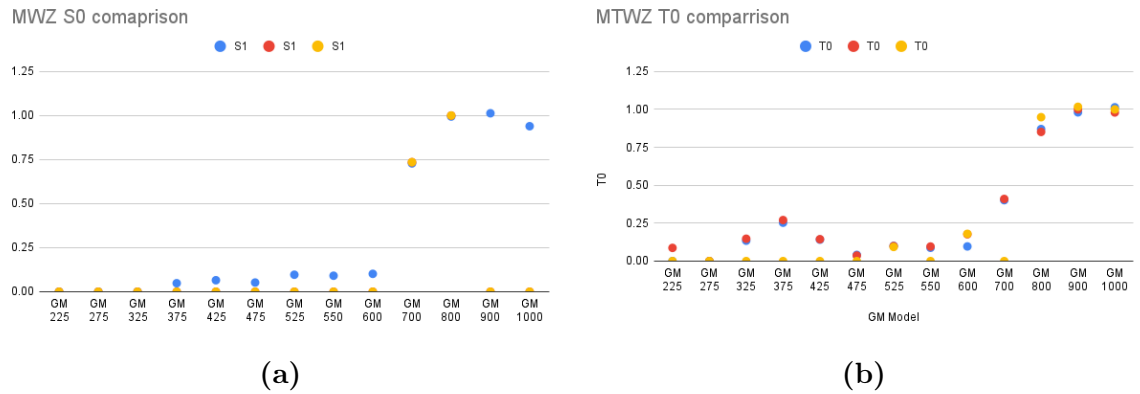


Figure 5.4: a) EFT coefficients significance for invariant Mass b) EFT coefficients significance for transverse Mass

Mass	$M(WZ)$					
	S1	M0	M1	T0	T1	T2
positive extrema						
800 GeV	[89,129]	[20,28.4]	[29,42.4]	[2.1,2.8]	[1.4,2.01]	[4.1,6.03]
900 GeV	[-10,76.8]	[1.1,17.2]	[-0.41,25.3]	no extrema	[-0.057,1.18]	[0.035,3.56]
1000 GeV	[-447,71.7]	[281,16.2]	[-207,23.6]	no extrema	[-0.5,1.1]	[-8.2,3.32]
negative extrema						
800 GeV	[-130,-90.4]	[-27,-18.4]	[-43,-29.6]	[-1.9,-1.11]	[-2.1,-1.48]	[-6.3,-4.37]
900 GeV	[-78,248]	[-16, -0.115]	[-26,0.329]	[-0.89,0.109]	[-1.3,0.0591]	[-3.8,0.186]
1000 GeV	[-73,1096]	[-15,5.52]	[-24,9.92]	[-0.81,0.231]	[-1.2,14.3]	[-3.6,1.04]

Mass	$M_T(WZ)$					
	S1	M0	M1	T0	T1	T2
positive extrema						
800 GeV	[75,113]	[16,24.2]	[24,36.2]	no extrema	[1.1,1.73]	[3.2,5.0]
900 GeV	[15,68.4]	[3.4,14.8]	[4.9,22.2]	no extrema	[0.22,1.06]	[0.6,3.06]
1000 GeV	[-19,64.7]	[220.45,14]	[-23,21]	no extrema	[-0.33,1.0]	[-0.45,2.89]
negative extrema						
800 GeV	[-115,-76.3]	[-24,-15.5]	[-36,-23.8]	[-1.5,-0.792]	[-1.5,-0.792]	[-5.2,-3.41]
900 GeV	[-70,-16.4]	[-14,-2.99]	[-22,-4.97]	[-0.77,-0.0389]	[-1.1,-0.256]	[-3.3,-0.798]
1000 GeV	[-66,78.6]	[-14,6.69]	[-21,82.6]	[-0.71,0.0189]	[-1.0,0.97]	[-3.1,37.9]

Table 5.1: Invariant mass lower and upper 95% confidence level limits for a fit with linear and quadratic operators in WZ with all other aQCD parameters set to zero

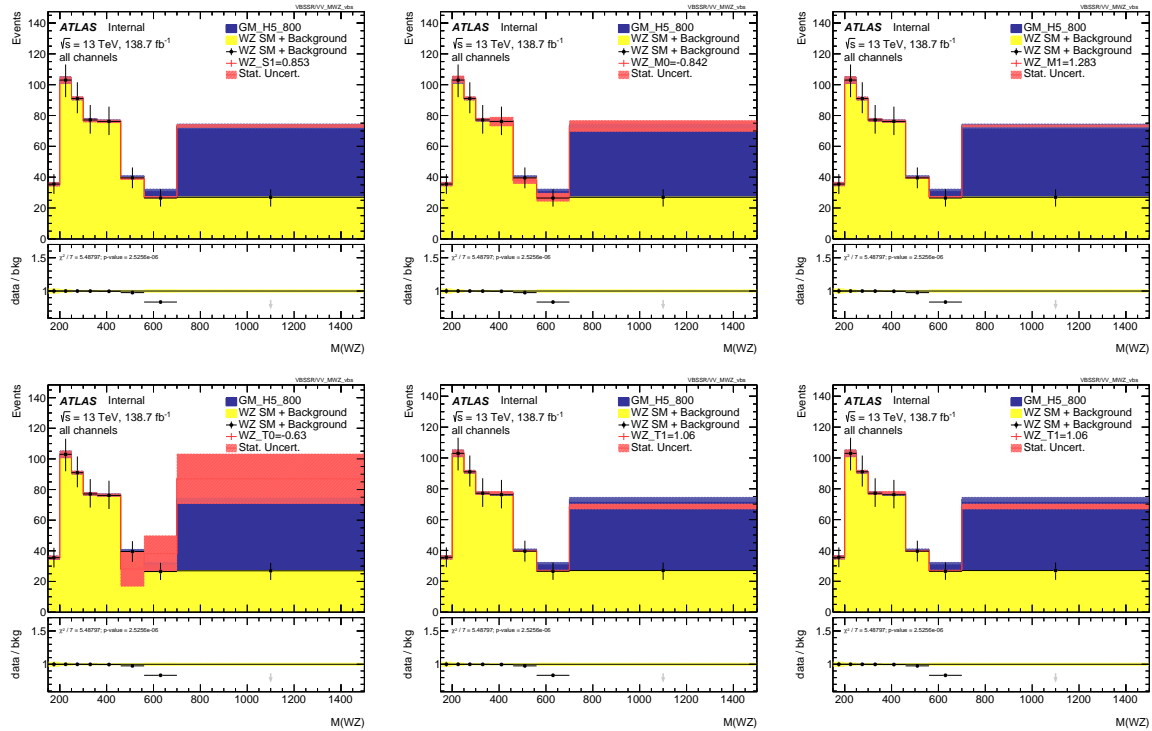


Figure 5.5: Invariant mass for parameters S1, M0, M1, T0, T1, T2 with best fit value for 800 GeV resonance

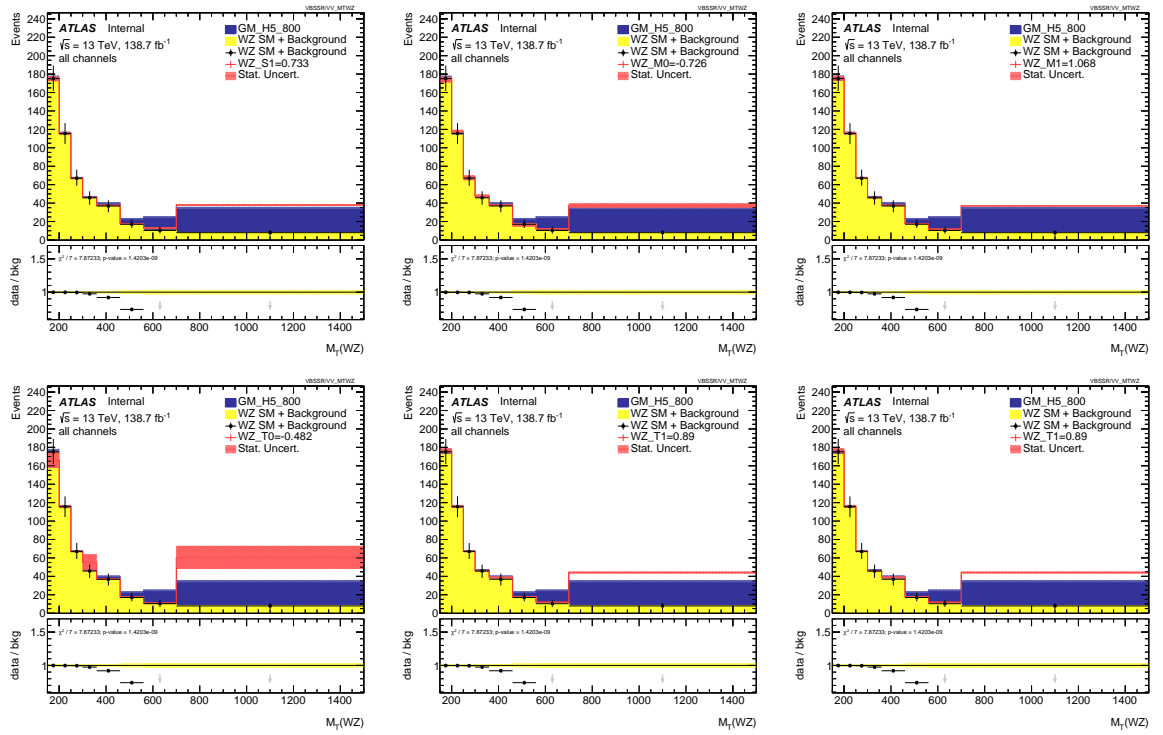


Figure 5.6: transverse mass for parameters S1, M0, M1, T0, T1, T2 with best fit value for 800 GeV resonance

6 Summery and Outlook

In this thesis the set out goal was to find the lowest energy resonance in WZ scattering process that can still be described using EFT. The results show that resonances with energy $E > 800$ GeV and an estimated minimum cross-section $\sigma_{resonance}$ of $92ab$ can be described accurately. The Limits for all relevant parameters S0, M0, M1, T0, T1, T2 for the research mass points with grater than 800 GeV are shown in table 5.1. These results are independent of the cross-section if the cross-section is grater than the minimum cross-section. Parameters showed a higher sensitivity for low cross-section in the transverse mass than in the invariant mass which required a cross-section $\sigma > 184ab$ as shon in figure 5.4.

This result is only valid for the sensitivity of dim-8 operates in WZ process, other VBS process may produce a different result. As the results are highly depend on binning further research with different binning depending on the resonance energy may be necessary since the same binning was used for all results. Only statistical uncertainties where used in this study including systematic uncertainties is needed for a more accurate prediction for the sensitivity of dim-8 operators.

In this thesis dim-6 operates are assumed to be negligible or gotten from another source which is often the case in EFT. This however may not always be true and needs further research the sensitivity of a combination of dim-6 and dim-8 operators for low energy resonance can not be predicted using these results. A next step in determining the sensitivity of dim-8 operators in VBS is to look at other VBS process which include different relevant operators. Another interesting research would be to use different models than the GM Model. EFT is Model independent the importance of matching the results to a BSM Model can not be overstated. Using other models will help to compare the Models and if a BSM interaction is found using EFT help matching the result to Ultraviolet Theory.

List of Figures

3.1	Sketch of the Basic EFT concept with the low energy observer having energy E and cutoff at Λ . The SM and BSM theory(here GM H5 Model) are combined in the Effective Field Theory. [Bri17]	11
3.2	a) Not all Models can be fitted using EFT only ones with energy scale higher than the SM b) Schematic of unitarity limits the energy range changes depending on the cutoff [MSz]	15
3.3	Comparison of interference term and quadratic term for the S1 parameters created with value S1=128. The quadratic term is bigger for higher energies since no unitarisation is used.	16
3.4	Interaction strength for different ranges of the Fundamental interactions. Although the Nuclear force isn't a fundamental it is shown in order to visualize point (c). [Teilchenwelt]	17
3.5	Example for SUSY as BSM Model. All particles shown here have been rejected as they should have been found using described methods in BSM search. []	18
3.6	Structure of Full VBS process $qq \rightarrow VVjj \rightarrow 4ljj$ with two of the four leptons having a charge. The circle stands for the processes a to e which come from the non-Abelian gauge group $SU(2)$ for weak interactions in leading order $VV \rightarrow VV$ processes.[Bit20]	19
3.7	Example Feynman diagrams for VVjj-EW6 processes. The dashed circle stands for the Feynman diagrams a-e in Figure 3.6	20
4.1	VBSSR region for a) invariant Mass, b) transverse mass. Showing reproduction of SM as well as the in section 3.3 discussed dominance of QCD and EW processes. VV, Vjets, Top, ttV, Vgamma, WZ_EWK , WZ_QCD are combined to ' $WZ_SM + Background$ ' in later plots. For the fits WZ_EWK is used as signal.	23

5.1	a) The invariant Mass of the resonance has approximately the same energy as the WZ peak but for the WZ peak the EFT prediction should be the SM therefore EFT can't describe the 225 GeV Resonance and the coefficient fit diverges. b) 700 GeV has a high cross-section and the energy is in the region where SM and EFT deviate therefore the coefficients can be fitted accurately. c) 1000 GeV the cross-section is to low the fit can produce a significant result even though the Resonance is in the right Energy region.	25
5.2	a) The best fit value is zero since the SM is reproduced in the asimov fit. c) The SM is excluded and two extrma emerge from the inclusion of the quadratic operator therm.	27
5.3	a) EFT coefficients significance for invariant Mass b) EFT coefficients significance for transverse Mass	27
5.4	a) EFT coefficients significance for invariant Mass b) EFT coefficients significance for transverse Mass	27
5.5	Invariant mass for parameters S1, M0, M1, T0, T1, T2 with best fit value for 800 GeV resonance	28
5.6	transverse mass for parameters S1, M0, M1, T0, T1, T2 with best fit value for 800 GeV resonance	29

List of Tables

4.1	Schematic view of cuts applied in different phase space regions. [Bit20]	21
4.2	Overwiev of Events in VBSSR region. mc16a is compared to the [STDM] for the reproduction of the SM EFT Limits. While the Resonance Fitting is done with the mc16e+mc16d data. The differences between the mc16a and the SM is like cause by some ELCORE settings since the cuts possible in the CAF tool where replicated.	23
4.3	Asmieve fit Limits for SM data with 95% CL. Differences arise from the use of mc16e, mc16d data compared to the mc16a data and the use of an BSM search optimized binning compared to the SM optimized binning used in [NEEd OSurce]	23
5.1	Invariant mass lower and upper 95% confidence level limits for a fit with linear and quadratic operators in WZ with all other aQCD parameters set to zero	28

Erklärung

Hiermit erkläre ich, dass ich diese Arbeit im Rahmen der Betreuung am Institut für ??? Physik ohne unzulässige Hilfe Dritter verfasst und alle Quellen als solche gekennzeichnet habe.

Vorname Nachname
Dresden, Monat 2019

6.1 Appendix